

R-Parity Violating Supersymmetry at HERA

E. Perez^a, Y. Sirois^b

^a CEN-Saclay, DSM/DAPNIA/SPP, Gif-sur-Yvette, France

^b LPNHE Ecole Polytechnique, IN2P3-CNRS, Palaiseau, France

H. Dreiner

Rutherford Appleton Laboratory, Chilton, Didcot, Oxon, United Kingdom

Abstract: The phenomenology and prospects for a discovery of R-parity violating Supersymmetry at HERA is analysed. Emphasis is put on the direct resonant production of squarks by electron-quark fusion and *all possible* subsequent decay modes of the squarks are considered. In particular, the full consequences of the mixing in the supersymmetric gaugino-higgsino sector are taken into account. A rich phenomenology emerges for HERA which offers a unique sensitivity to new R-parity violating couplings and good discriminating power against free parameters of the theory.

1 Introduction

Supersymmetry (SUSY) which fundamentally links fermions and bosons is likely to be chosen as an essential property of a true theory beyond the Standard Model (SM). Among the most compelling arguments for a SUSY world are the fact that local supersymmetric transformations are fundamentally related to generators of space-time translation (hence necessarily incorporates gravity) [1], the possibility to “explain” the hierarchy between the electroweak mass scale and the Grand Unification or Planck mass scale, and the stability of a softly broken SUSY which “naturally” avoids the arbitrary fine tuning of the parameters which is necessary in the SM [2].

A natural framework for SUSY searches is provided by the Minimal Supersymmetric extension of the Standard Model (MSSM) [3] which has predictive power within a finite and well defined set of free parameters and has neither been proven nor falsified by experimental observations. The latter is a non-trivial status given the remarkable precision tests of the SM at the LEP collider over the recent years. It might have to do with the fact that quantum corrections due to the sparticles which otherwise respect all gauge symmetries of the SM tend to be small rendering indirect observations difficult. It is in addition possible that direct searches for particles of the minimal field representation offered by the MSSM have at least partly failed because they were looking at the wrong phenomenology.

The most general Yukawa couplings in a supersymmetric theory which is gauge invariant and minimal in terms of field content can be written [4] in the compact formalism of the

superpotential as $W_{SUSY} = W_{MSSM} + W_{\mathcal{R}_p}$. The W_{MSSM} contains terms which are responsible for the Yukawa couplings of the Higgs fields to ordinary fermions. The $W_{\mathcal{R}_p}$ is given by:

$$W_{\mathcal{R}_p} = \lambda_{ijk} L_i L_j \bar{E}_k + \lambda'_{ijk} L_i Q_j \bar{D}_k + \lambda''_{ijk} \bar{U}_i \bar{D}_j \bar{D}_k \quad (1)$$

where ijk are generation indices of the superfields L, Q, E, D and U . The L and Q are left-handed doublets while \bar{E}, \bar{D} and \bar{U} are right-handed singlet superfields for charged leptons, down and up-type quarks, respectively. The λ and λ' terms induce lepton number violation while the λ'' terms induce baryon number violation. In the strict MSSM framework, one imposes that the SUSY theory be also minimal in terms of allowed couplings and all $W_{\mathcal{R}_p}$ terms are avoided by imposing a strict conservation of the R-parity defined as $R_p = (-1)^{3B+L+2S} = 1$ (for particles) $= -1$ (for sparticles), where S denotes the spin, B the baryon number and L the lepton number. Imposing this discrete symmetry is a somewhat *ad hoc* prescription. Another viable [5] and less restrictive discrete symmetry is the B -parity which imposes only baryon number conservation (i.e. $\lambda'' = 0$). Vanishing λ'' couplings is sufficient to avoid unacceptable $n - \bar{n}$ oscillations and fast proton decay. Moreover from the cosmological point of view, the observed matter/antimatter asymmetry imposes much more severe constraints on λ'' than on λ or λ' [6]. Finally, B -parity is favoured over R -parity conservation in a large class of superstring inspired models [5]. It is also interesting to note that the λ and λ' terms in (1) which have no equivalent in the SM arise in a fundamental way from the fact that $SU(2)$ -doublet lepton superfields have the same gauge quantum numbers as the Higgs supermultiplets.

The ep collider HERA which provides both leptonic and baryonic quantum numbers in the initial state is ideally suited for \mathcal{R}_p searches. This was realized long ago and was first investigated theoretically in the context of the previous HERA Workshop [7] which motivated early experimental searches [8]. The cases $\lambda' \neq 0$ which could lead to resonant production of squarks via e - q fusion offers of course the most exciting prospects. Recent investigations [9, 10, 11] have shown that a new and rich phenomenology (different for e^- and e^+ beams) emerges when considering the full complexity of the mixing in the gaugino-higgsino sector of the theory. This is studied in more details in this contribution in view of future high luminosity runs at HERA.

The case of associated \tilde{e} - \tilde{q} production at HERA followed by the \mathcal{R}_p -decay of the sfermions has already been studied in detail and also in view of high luminosity runs at HERA in [12]. Via this process one can probe significantly smaller Yukawa couplings than via the resonant production but only at smaller sfermion masses.

2 Phenomenology of \mathcal{R}_p SUSY

2.1 Modelling and Free Parameters

The $\lambda'_{ijk} L_i Q_j \bar{D}_k$ terms in the \mathcal{R}_p extension of the MSSM correspond in expanded field notation to the Lagrangian

$$\begin{aligned} \mathcal{L}_{L_i Q_j \bar{D}_k} = & \lambda'_{ijk} \left[-\tilde{e}_L^i u_L^j \bar{d}_R^k - e_L^i \tilde{u}_L^j \bar{d}_R^k - (\bar{e}_L^i)^c u_L^j \tilde{d}_R^{k*} \right. \\ & \left. + \tilde{\nu}_L^i d_L^j \bar{d}_R^k + \nu_L d_L^j \bar{d}_R^k + (\bar{\nu}_L^i)^c d_L^j \tilde{d}_R^{k*} \right] + \text{h.c.} \end{aligned} \quad (2)$$

where the superscripts c denote the charge conjugate spinors and the $*$ the complex conjugate of scalar fields. Among the 27 possible λ'_{ijk} couplings, the cases $i = 1$ can lead to direct squark resonant production and are thus of special interest at HERA. These cases are studied first in this paper assuming conservatively that one of the λ' dominates.

The masses of the scalar quarks and scalar leptons, bosonic sparticle partners of the SM fermions, are treated here as free parameters. In the gaugino-higgsino sector, there are four neutralinos χ_i^0 ($i = 1 \dots 4$) which are mixed states of the photino $\tilde{\gamma}$, the zino \tilde{Z} and the supersymmetric partners \tilde{H}_1^0 and \tilde{H}_2^0 of the two neutral Higgs fields. Two charginos χ_j^\pm ($j = 1, 2$) are mixed states of the winos \tilde{W}^\pm and of the SUSY partners of the charged Higgs fields. The masses and couplings of the χ^0 and χ^\pm are calculated in terms of the MSSM basic parameters :

- M_1 and M_2 , the $U(1)$ and $SU(2)$ soft-breaking gaugino mass terms;
- μ , the Higgs mixing parameter;
- $\tan \beta$, the ratio of the vacuum expectation values of the two neutral Higgs fields.

The number of free parameters is reduced by assuming a relation at the Grand Unification (GUT) scale between M_1 and M_2 (see Appendix for detail). No other GUT relations are used and in particular the gluino (\tilde{g}) mass is left free.

We moreover consider the following simplifying assumptions :

- all squarks (except the stop) are quasi-degenerate in mass;
- the lightest supersymmetric particle (LSP) is the lightest neutralino χ_1^0 ;
- gluinos are heavier than the squarks such that decays $\tilde{q} \rightarrow q + \tilde{g}$ are kinematically forbidden.

It should be made clear that there are no compelling cosmological constraints in \mathcal{R}_p models which impose that the LSP be neutral and colourless. Other possible choices for the LSP (e.g. \tilde{g} or χ^\pm) would not significantly change the search and analysis strategy and will only be briefly discussed. In \mathcal{R}_p models, in contrast to the strict MSSM, the LSP is generally unstable. This leads to event topologies which differ strongly from the characteristic “missing energy” signal due to LSP’s escaping detection in the MSSM. Hence, except for exclusion limits derived from indirect searches (e.g. from the intrinsic width of the Z^0), the mass constraints obtained in the MSSM framework do not apply directly in \mathcal{R}_p models. The search for \mathcal{R}_p squarks is “complementary” (hence mandatory) to that performed in the strict MSSM framework.

2.2 Squark Production

The resonant squark production mode through direct e - q fusion is illustrated in Fig. 1 for $\lambda'_{111} \neq 0$. By gauge symmetry, only \tilde{u}_L -like or \tilde{d}_R -like squarks (or their charge conjugates) can be produced in ep collisions. The production of “left” squarks (i.e. supersymmetric partners of left-handed quarks) is the dominating process if HERA delivers positrons, since the fusion occurs via a d valence quark. On the contrary, with electrons in the initial state, mainly “right” squarks are produced. This dichotomy has important consequences since “left” and

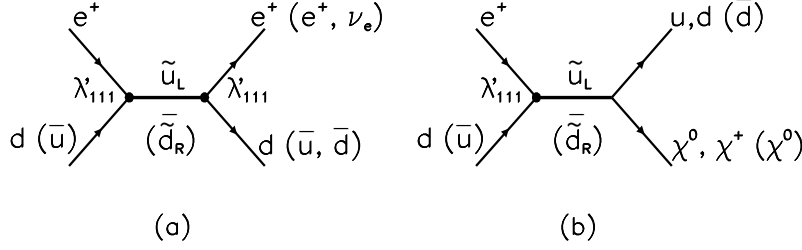


Figure 1: R_p resonant production of \tilde{u}_L or \tilde{d}_R squarks in e^+p collisions with subsequent (a) R_p decay or (b) gauge decay involving a (generally) unstable gaugino-higgsino (χ^0 or χ^+).

“right” squarks have different allowed or dominant decay modes as will be seen in the following sections. In particular, new exotic final state topologies might have sizeable contributions in e^+p collisions.

HERA offers a high sensitivity to any of the nine λ'_{1jk} couplings, in contrast to most indirect processes. The production processes allowed for each λ'_{1jk} are listed in Table 1 for an e^+ beam. Squark production via λ'_{1j1} is especially interesting in e^+p collisions as it involves a valence d quark, whilst λ'_{11k} are best probed with an e^- beam since squark production then involves a valence u quark.

Figure 2 shows the production cross-sections via λ'_{111} for \tilde{u}_L and \tilde{d}_R , and for \tilde{c}_L via λ'_{121} , each plotted for coupling values of $\lambda' = 0.1$. In the narrow width approximation, these cross-sections are simply expressed as

$$\sigma_{\tilde{q}} = \frac{\pi}{4s} \lambda'^2 q' \left(\frac{M^2}{s} \right) \quad (3)$$

where $\sqrt{s} = \sqrt{4E_e^0 E_p^0} \simeq 300$ GeV is the energy available in the CM frame for incident beam energies of $E_e^0 = 27.5$ GeV and $E_p^0 = 820$ GeV, and $q'(x)$ is the probability to find the relevant quark (e.g. the d for \tilde{u}_L or \tilde{c}_L and the \bar{u} for \tilde{d}_R) with momentum fraction $x = M^2/s \simeq M_q^2/s$ in

λ'_{1jk}	Production processes	
111	$e^+ + \bar{u} \rightarrow \tilde{d}_R$	$e^+ + d \rightarrow \tilde{u}_L$
112	$e^+ + \bar{u} \rightarrow \tilde{s}_R$	$e^+ + s \rightarrow \tilde{u}_L$
113	$e^+ + \bar{u} \rightarrow \tilde{b}_R$	$e^+ + b \rightarrow \tilde{u}_L$
121	$e^+ + \bar{c} \rightarrow \tilde{d}_R$	$e^+ + d \rightarrow \tilde{c}_L$
122	$e^+ + \bar{c} \rightarrow \tilde{s}_R$	$e^+ + s \rightarrow \tilde{c}_L$
123	$e^+ + \bar{c} \rightarrow \tilde{b}_R$	$e^+ + b \rightarrow \tilde{c}_L$
131	$e^+ + \bar{t} \rightarrow \tilde{d}_R$	$e^+ + d \rightarrow \tilde{t}_L$
132	$e^+ + \bar{t} \rightarrow \tilde{s}_R$	$e^+ + s \rightarrow \tilde{t}_L$
133	$e^+ + \bar{t} \rightarrow \tilde{b}_R$	$e^+ + b \rightarrow \tilde{t}_L$

Table 1: Squark production processes at HERA (e^+ beam) via a R -parity violating λ'_{1jk} coupling.

the proton. Hence the production cross-section approximately scales in λ'^2 . The full kinematic domain can be probed at HERA for couplings weaker than the electromagnetic coupling (i.e. $\lambda^2/4\pi < \alpha_{em}$) given an integrated luminosity of $\simeq 500\text{pb}^{-1}$.

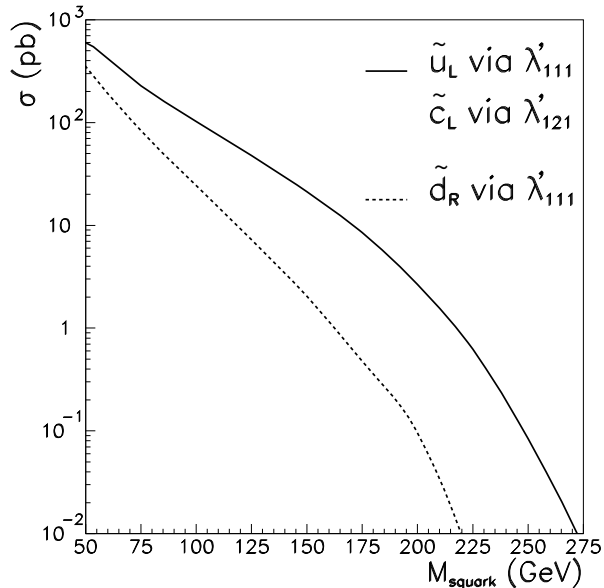


Figure 2: Squark production cross-sections in e^+p collisions for a coupling $\lambda'_{1j1} = 0.1$.

2.3 Squark Decays

The squarks decay either via their Yukawa coupling into ordinary matter fermions, or in a first step via their gauge coupling into a quark and a neutralino χ_i^0 ($i = 1 \dots 4$) or a chargino χ_j^\pm ($j = 1, 2$). The former modes are henceforward called “squark \mathcal{R}_p decays” and the latter “squark gauge decays”.

\mathcal{R}_p decays of squarks:

In cases where both production and decay occurs through a λ'_{1jk} coupling (e.g. Fig. 1a for $\lambda'_{111} \neq 0$), the squarks behave as scalar leptoquarks [13, 14]. For $\lambda'_{111} \neq 0$, the \tilde{d}_R resembles on event-by-event the \tilde{S}^0 leptoquark and decays in either $e^+ + \bar{u}$ or $\nu_e + \bar{d}$ while the \tilde{u}_L resembles the $\tilde{S}_{1/2}$ and only decays into $e^+ \bar{d}$. The partial decay width reads :

$$\Gamma_{\tilde{q} \rightarrow \mathcal{R}_p} = \Gamma_{\tilde{u}_L \rightarrow e^+ d} = \Gamma_{\tilde{d}_R \rightarrow e^+ \bar{u}} = \Gamma_{\tilde{d}_R \rightarrow \nu_e \bar{d}} = \frac{1}{16\pi} \lambda'_{111}{}^2 M_{\tilde{q}} \quad (4)$$

so that squark \mathcal{R}_p decays will mainly contribute at high mass for large Yukawa coupling values λ' . Hence, the final state signatures consist of a lepton and a jet and are, event-by-event, indistinguishable from the SM neutral (NC) and charged current (CC) deep inelastic scattering (DIS).

Gauge decays of squarks:

The MSSM Lagrangian contains terms coupling a sfermion to an ordinary fermion and a gaugino-higgsino. The partial widths for squark gauge decays depend on MSSM parameters via the composition of the neutralinos or charginos.

Both \tilde{q}_L and \tilde{q}_R squarks can decay via $\tilde{q} \rightarrow q\chi_i^0$. The partial width of the $\tilde{q} \rightarrow q\chi_i^0$ decay is calculated to be

$$\Gamma_{\tilde{q} \rightarrow q + \chi_i^0} = \frac{1}{8\pi} (A^2 + B^2) M_{\tilde{q}} \left(1 - \frac{M_{\chi_i^0}^2}{M_{\tilde{q}}^2} \right)^2 \quad (5)$$

where :

$$A = \frac{gM_q N_{i4}}{2M_W \sin \beta} \quad , \quad B = ee_q N'_{i1} + g(0.5 - e_q \sin^2 \theta_W) \frac{N'_{i2}}{\cos \theta_W}, \quad (6)$$

and where N_{ij} (N'_{ij}) is the transport matrix which diagonalizes the neutralino mass matrix (see Appendix for detail) in the $\tilde{A} - \tilde{W}_3$ ($\tilde{\gamma} - \tilde{Z}$ basis). In practice, the χ_i^0 masses and the exact values of the ‘‘chiral’’ couplings A and B depend on the relative $\tilde{\gamma}$, \tilde{Z} and \tilde{H} components of the χ_i^0 .

The dependence of the χ_i^0 mass on the μ parameter is shown in Fig. 3a for fixed M_2 and $\tan \beta$. The dominant component ($\tilde{\gamma}$, \tilde{Z} or \tilde{H}) of the lightest state χ_1^0 is shown in Fig. 3b. More

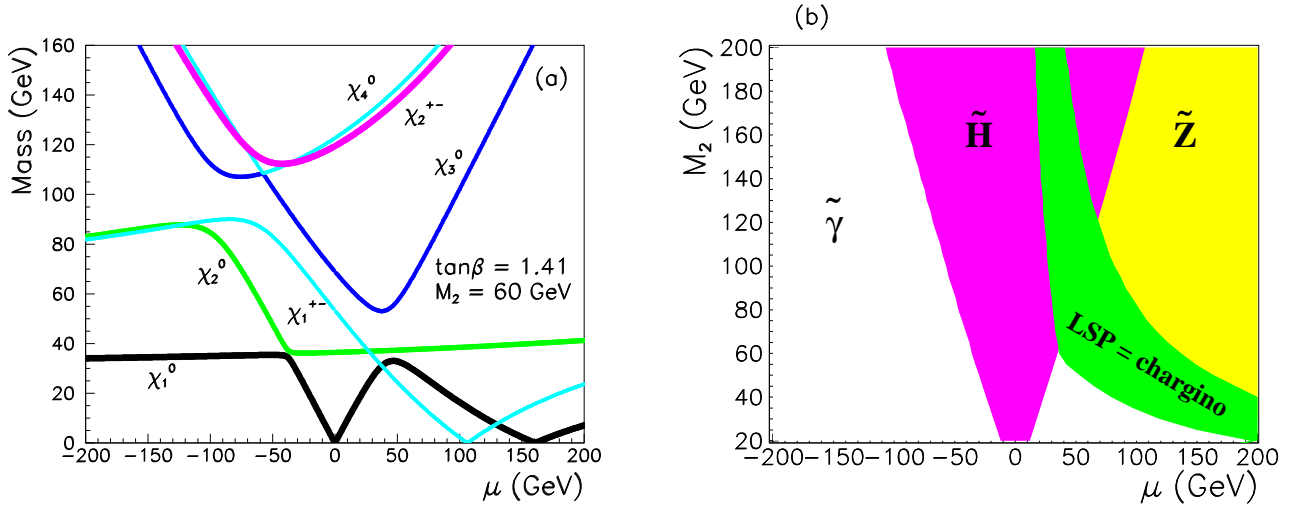


Figure 3: (a) Physical masses of the χ_i^0 and χ_i^\pm as a function of μ for $\tan \beta = 1$ and $M_2 = 60$ GeV; (b) Main component of the LSP for $\tan \beta = 1$

details on the way the nature (and masses) of the various neutralino states depend on the basic MSSM parameters M_2 , μ and $\tan \beta$ can be found in the Appendix.

For a $\tilde{\gamma}$ -like LSP, i.e. a χ_1^0 dominated by its photino component, the \tilde{q} to $q + \tilde{\gamma}$ coupling is proportional to the q electric charge and the \tilde{q} partial width reduces to

$$\Gamma_{\tilde{q} \rightarrow q + \tilde{\gamma}} = \frac{1}{8\pi} e^2 e_q^2 M_{\tilde{q}} \left(1 - \frac{M_{\tilde{\gamma}}^2}{M_{\tilde{q}}^2} \right)^2. \quad (7)$$

In such a case, more than 90% of the $\tilde{q} \rightarrow q\chi_i^0$ decays will involve the χ_1^0 . A similar partial branching ratio holds for a \tilde{H} -like LSP with a relatively large \tilde{Z} component (e.g. in the \tilde{H} region close to the \tilde{Z} region in Fig. 3b). For a \tilde{Z} -like LSP, this branching ratio reduces to $20\% < \mathcal{B} < 80\%$. Decays involving the LSP are negligible only in the \tilde{H} domain extending to negative μ 's adjacent to the $\tilde{\gamma}$ domain (Fig. 3b).

(Almost) only the \tilde{q}_L are allowed by gauge symmetry to decay into $q'\chi_i^+$. This is because the $SU(2)_L$ symmetry which implies in the SM that the right handed fermions do not couple to the W boson also forbids a coupling of \tilde{q}_R to the \tilde{W} . The \tilde{q}_R decays involving the chargino is only possible through the \tilde{H}^+ component of the χ^+ in which case the coupling is proportional to the q' mass. Hence the decay $\tilde{q}_R \rightarrow q'\chi_i^+$ is strongly suppressed for a \tilde{q}_R of the first or second generation. The partial width of the $\tilde{q} \rightarrow q\chi_i^+$ decay is obtained from (5) with the interchange $M_{\chi_i^0} \rightarrow M_{\chi_i^+}$ and with :

$$A = \frac{gV_{i1}}{\sqrt{2}} \quad B = \frac{-gM_{q'}U_{i2}}{2M_W \cos \beta}. \quad (8)$$

The regions of the M_2 vs μ plane where the \tilde{u} decays involving a chargino dominate are shown in Fig. 4. In most of the parameter space, the \tilde{u}_L squarks will mainly undergo a decay involving

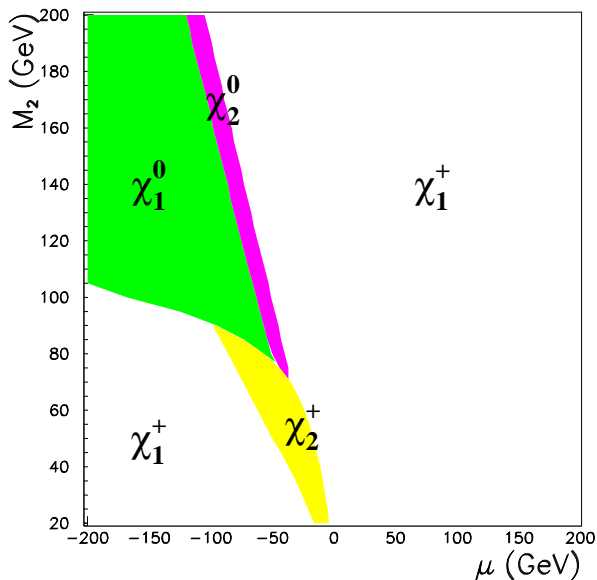


Figure 4: Dominant gauge decay of a 150 GeV \tilde{u}_L squark.

a chargino if kinematically allowed. The mass dependence of the χ_i^+ states on the μ parameter is shown in Fig. 3a for fixed M_2 and $\tan \beta$.

2.4 Decays of the LSP

In \mathcal{R}_p SUSY models with $\lambda'_{1jk} \neq 0$, the LSP will undergo one of the following decays : $\chi_1^0 \rightarrow \nu \bar{d}_k d$, $\chi_1^0 \rightarrow e^+ \bar{u}_j d_k$ or $\chi_1^0 \rightarrow e^- u_j \bar{d}_k$. Representative diagrams of such decays are given in Fig. 5. The relevant matrix elements for these decays can be found in [12]. They depend on the coupling λ' , but also on the parameters M_2 , μ and $\tan \beta$. This dependence is illustrated in Fig. 6a for the LSP decay $\chi_1^0 \rightarrow e^\pm q \bar{q}'$. Such decay modes are seen to be dominant ($63\% < \mathcal{B}_R < 88\%$) if the χ_1^0 is $\tilde{\gamma}$ -like in which case both the “right” and the “wrong” sign lepton (compared to the incident beam) are equally probable. This leads to largely background free striking signatures for lepton number violation. The latter will dominate if the χ_1^0 is \tilde{Z} -like. A \tilde{H} -like χ_1^0 will most probably be long lived and escape detection since its coupling to fermion-sfermion pairs is proportional to the fermion mass [15]. This is illustrated in Fig. 6b, which shows the flight distance $c\tau_0$ of

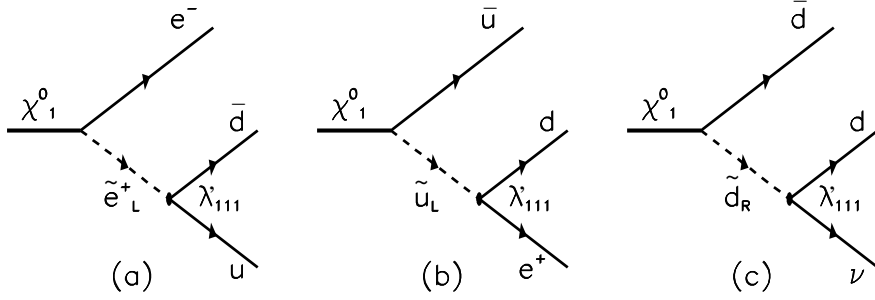


Figure 5: *Example diagrams of the LSP decays $\chi_1^0 \rightarrow lqq'$ involving a \tilde{R}_p Yukawa coupling.*

the χ_1^0 in the plane (M_2, μ) for $\lambda' = 0.1$. The $c\tau_0$ exceeds 1 m in most of the \tilde{H} -like domain surrounding the singularity at $\mu = 0$ where $M_{\chi_1^0} = 0$ at tree level. Hence processes involving a higgsino-like χ_1^0 will be affected by an imbalance in transverse momenta.

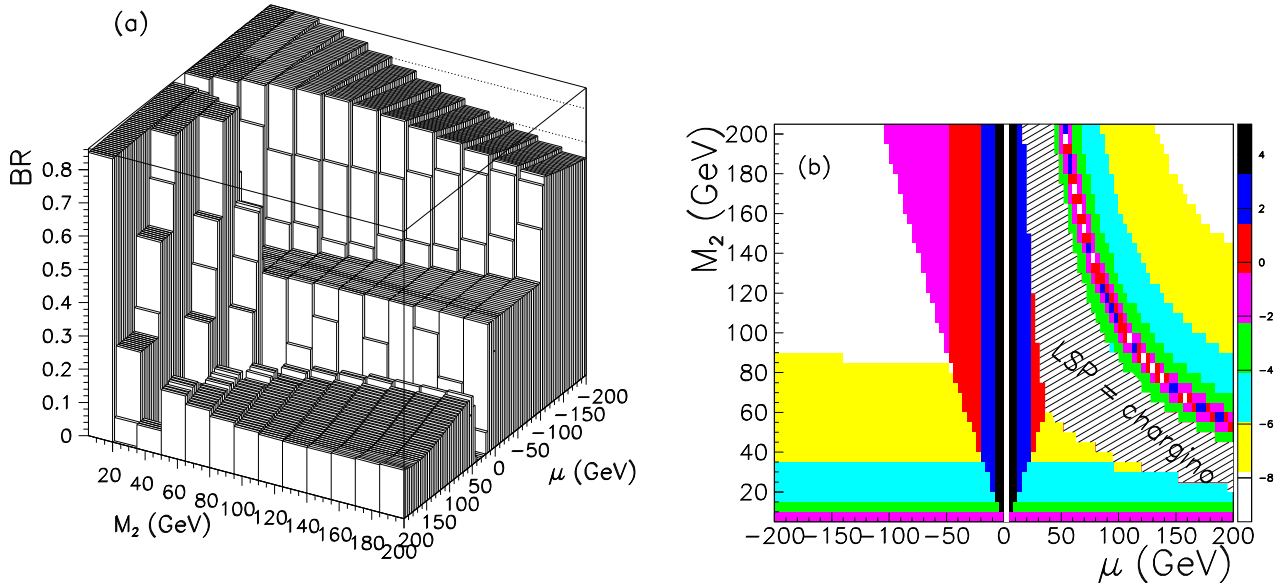


Figure 6: (a) *LSP (χ_1^0) decay branching ratio into charged leptons (i.e. $e^\pm + jets$), as a function of μ and M_2 for sfermion masses $M_{\tilde{f}} = 150$ GeV and $\tan\beta = 1$; (b) $\log c\tau_0$ (m) of the LSP with $\lambda' = 0.1$, the LSP mass is vanishingly small around $\mu = 0$ and along the ridge at large $\mu + M_2$.*

2.5 Decays of Charginos

R-parity conserved χ^+ decays into a χ^0 and two matter fermions, have been investigated in detail in [16], where the relevant matrix elements can be found. New decay modes of the χ^+ into $e^+ + d_j + \bar{d}_k$ or $\nu_e + u_j + \bar{d}_k$ are allowed by the \tilde{R}_p couplings λ'_{1jk} as illustrated in Fig. 7.

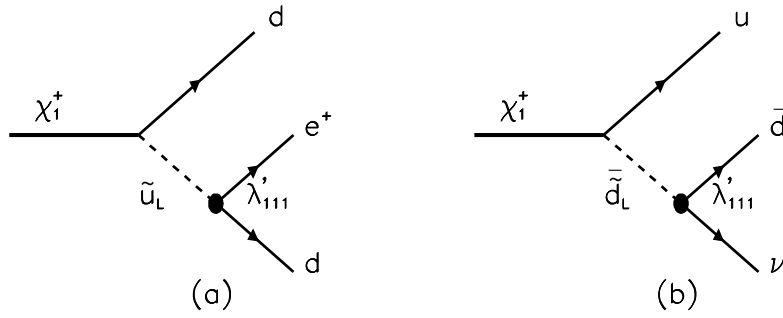


Figure 7: *Representative diagrams for the χ_1^+ decays $\chi_1^+ \rightarrow lqq'$ involving a \mathcal{R}_p Yukawa coupling.*

The branching ratio of the χ_1^+ into these \mathcal{R}_p modes is obtained using the partial widths calculated from the relevant matrix elements. Considering for instance the process $\chi_1^+ \rightarrow e^+ + d_j + \bar{d}_k$ (Fig. 7a) in the following notation $\chi_1^+(k) \rightarrow e^+(l) + \bar{d}(q_1) + d(q_2)$, and using Mandelstam variables $s = (q_1 + q_2)^2 = (k - l)^2$, $t = (k - q_1)^2 = (l + q_2)^2$ and $u = (k - q_2)^2 = (l + q_1)^2$, the squared matrix element can be written as :

$$|\mathcal{M}|_{\mathcal{R}_p}^2 = 3g^2\lambda'_{111}{}^2|V_{11}|^2 \left(\frac{s(M_\chi^2 - s)}{|R(s)|^2} + \frac{t(M_\chi^2 - t)}{|D(t)|^2} - \mathcal{R}e \frac{I(s, t, u)}{R(s)D(t)} \right) \quad (9)$$

where the propagators R and D and the interference term I are :

$$R(s) = s - m_{\tilde{\nu}_L}^2, \quad (10)$$

$$D(t) = t - m_{\tilde{u}_L}^2, \quad (11)$$

$$I(s, t, u) = s(M_\chi^2 - s) - u(M_\chi^2 - u) + t(M_\chi^2 - t). \quad (12)$$

The matrix element corresponding to the process $\chi_1^+ \rightarrow \nu_e + u + \bar{d}$ (Fig. 7b) is deduced from the previous one with the following substitutions: $e \rightarrow \nu$, $\bar{d} \rightarrow u$, $d \rightarrow \bar{d}$ and $|V_{11}|^2 \rightarrow |U_{11}|^2$. The corresponding partial width is obtained by integrating over phase space as :

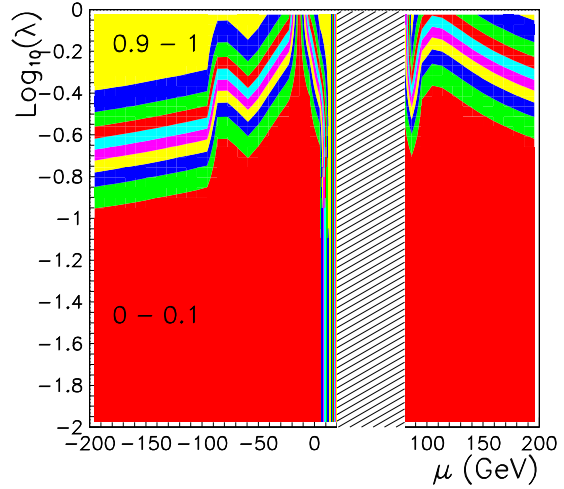
$$\Gamma = \int_{s=0}^{s=M_{\chi_1^+}^2} \int_{t=0}^{t=M_{\chi_1^+}^2 - s} \frac{1}{M_{\chi_1^+}^3} \frac{1}{256\pi^3} |\mathcal{M}|^2 ds dt \quad (13)$$

The \mathcal{R}_p decays of the χ_1^+ will mainly dominate over MSSM decays as soon as λ' is not too small, as can be seen in Fig. 8. For $\chi_1^0 \simeq \tilde{\gamma}$, \mathcal{R}_p decays of the chargino dominate over MSSM modes for coupling values above $\simeq 0.25$, which is typically HERA's sensitivity limit with current luminosity.

2.6 Classification of Final States

Taking into account the dependence on the nature of the χ_1^0 , the possible decay chains of the \tilde{u}_L and \tilde{d}_R squarks can be classified into eight distinguishable event topologies listed in tables 2 and 3 and labelled S1 to S8. The S1 and S2 classes cover \mathcal{R}_p squark decays. The S3 and S4 classes are squark gauge decay topologies not accompanied by escaping transverse momenta

Figure 8: \mathcal{R}_p chargino decay branching ratio as a function of λ'_{111} and μ , for $M_2 = 80$ GeV, $\tan\beta = 1$ and sfermions masses = 150 GeV; the hatched domain corresponds to μ values for which $M(\chi_1^+) < M(\chi_1^0)$.



Channel	χ_1^0 nature	Decay processes	Signature
S1	$\tilde{\gamma}, \tilde{Z}, \tilde{H}$	$\tilde{q} \xrightarrow{\lambda'} e^+ q'$	High $P_\perp e^+ + 1$ jet
S2	$\tilde{\gamma}, \tilde{Z}, \tilde{H}$ \tilde{H}	$\tilde{d}_R \xrightarrow{\lambda'} \nu_e \bar{d}$ $\tilde{q} \longrightarrow q \chi_1^0$	Missing $P_\perp + 1$ jet
S3	$\tilde{\gamma}, \tilde{Z}$ $\tilde{\gamma}, \tilde{Z}, \tilde{H}$ $\tilde{\gamma}, \tilde{Z}$	$\tilde{q} \longrightarrow q \chi_1^0$ $\xrightarrow{\lambda'} e^+ \bar{q}' q''$ $\tilde{u}_L \longrightarrow d \chi_1^+$ $\xrightarrow{\lambda'} e^+ d \bar{d}$ $\tilde{u}_L \longrightarrow d \chi_1^+$ $\hookrightarrow W^+ \chi_1^0$ $\xrightarrow{\lambda'} e^+ \bar{q}' q''$ $\hookrightarrow q \bar{q}'$	High $P_\perp e^+$ + multiple jets
S4	$\tilde{\gamma}, \tilde{Z}$ $\tilde{\gamma}, \tilde{Z}$	$\tilde{q} \longrightarrow q \chi_1^0$ $\xrightarrow{\lambda'} e^- \bar{q}' q''$ $\tilde{u}_L \longrightarrow d \chi_1^+$ $\hookrightarrow W^+ \chi_1^0$ $\xrightarrow{\lambda'} e^- \bar{q}' q''$ $\hookrightarrow q \bar{q}'$	High $P_\perp e^-$ (i.e. wrong sign lepton) + multiple jets

Table 2: Squark decays in \mathcal{R}_p SUSY classified per distinguishable event topologies (PART I). The dominant component of the χ_1^0 for which a given decay chain is relevant is given in the second column. The list of processes contributing to a given event topology is here representative but not exhaustive.

\mathcal{P}_\perp , while those with large \mathcal{P}_\perp are covered by classes S5 to S8. A set of event selection cuts has been developed and discussed in detail in [8, 11].

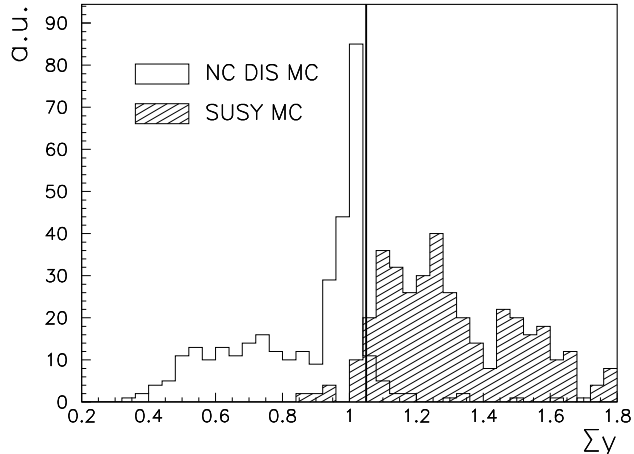
Channel	χ_1^0 nature	Decay processes	Signature
S5	$\tilde{\gamma}, \tilde{Z}$	$\tilde{q} \longrightarrow q \chi_1^0$ $\xrightarrow{\chi'} \nu \bar{q}' q'$	Missing P_\perp + multiple jets
	$\tilde{\gamma}, \tilde{Z}$	$\tilde{u}_L \longrightarrow d \chi_1^+$ $\hookrightarrow W^+ \chi_1^0$ $\xrightarrow{\chi'} \nu \bar{q}' q'$ $\hookrightarrow q \bar{q}'$	
	$\tilde{\gamma}, \tilde{Z}, \tilde{H}$	$\tilde{u}_L \longrightarrow d \chi_1^+$ $\xrightarrow{\chi'} \nu u \bar{d}$	
	\tilde{H}	$\tilde{u}_L \longrightarrow d \chi_1^+$ $\hookrightarrow W^+ \chi_1^0$ $\hookrightarrow q \bar{q}'$	
S6	\tilde{H}	$\tilde{u}_L \longrightarrow d \chi_1^+$ $\hookrightarrow W^+ \chi_1^0$ $\hookrightarrow l^+ \nu$	High $P_\perp e^+$ or μ^+ + missing P_\perp + 1 jet
S7	$\tilde{\gamma}, \tilde{Z}$	$\tilde{u}_L \longrightarrow d \chi_1^+$ $\hookrightarrow W^+ \chi_1^0$ $\xrightarrow{\chi'} e^\pm \bar{q}' q''$ $\hookrightarrow l^+ \nu$	High $P_\perp e^\pm$ + high $P_\perp e^+$ or μ^+ + missing P_\perp + multiple jets
S8	$\tilde{\gamma}, \tilde{Z}$	$\tilde{u}_L \longrightarrow d \chi_1^+$ $\hookrightarrow W^+ \chi_1^0$ $\xrightarrow{\chi'} \nu \bar{q}' q'$ $\hookrightarrow l^+ \nu$	High $P_\perp e^+$ or μ^+ + missing P_\perp + multiple jets

Table 3: *Squark decays in \mathbb{R}_p SUSY classified per distinguishable event topologies (Part II). As in table 2, the list of processes given here is not exhaustive, e.g. the gauge decays $\chi_1^+ \rightarrow \chi_1^0 l^+ \nu$ and $\chi_1^+ \rightarrow \chi_1^0 q \bar{q}'$ may also proceed via a virtual sfermion.*

For S1 and S3 (or S4), the DIS NC background is strongly suppressed by requiring a high $P_\perp e^\pm$ found at high y_e , where $y_e = 1/2(1 + \cos \theta_e^*)$ and θ_e^* is the electron angle in the $e - q$ CM frame. The uniform decay of the scalar particle in the CM frame leads to a flat y_e spectrum for S1 and one shifted towards largest y_e for S3. This is in contrast to the $1/y_e^2$ spectrum expected for the DIS NC background at fixed quark momentum fraction x . For S3 the H1 analysis [11] has been improved [17], using θ^* 's computed for the scattered electron and for the highest P_\perp jet found in the azimuthal hemisphere opposite to the electron, and cutting on $\Sigma y = y_e + y_{jet}$ as shown in Fig. 9. Good signal detection efficiencies are obtained in each of these classes, reaching $\sim 70\%$ for S1 and up to $\sim 60\%$ depending on $M_{\chi_1^0}$ for S3.

The S4 topology with a wrong sign lepton in the final state is quasi-background free. Event candidates in classes S2 and S5 to S8 have a large P_\perp . Classes S2 and S5 suffer from DIS CC background and from tails of photoproduction background. The S6 to S8 topologies have one or many leptons in the final states and are thus quasi-background free. Typical signal detection efficiencies [11] reach $\sim 30\% \rightarrow 80\%$ in these channels.

Figure 9: *Distribution of the variable Σy for neutral current DIS processes, and for a simulation of 75 GeV squarks undergoing gauge decays involving 20 GeV neutralinos; the vertical line is the cut used in the H1 analysis [17].*



The relative contributions of the squark \mathcal{R}_p and gauge decays are shown in Fig. 10a. Gauge decays are seen to dominate through most of the accessible mass range. Only large Yukawa couplings can be probed at largest masses and thence \mathcal{R}_p decays dominate. The shape of the curves in Fig. 10a is only distorted at lowish mass (e.g. $M_{\tilde{q}} \lesssim 75$ GeV) when convoluting with signal detection efficiencies. The measurement of the relative branching ratio in $S3$ and $S4$ in case of a discovery, could be used to constrain the χ_1^0 LSP nature in the MSSM parameter space as seen in Fig. 10b.

It is interesting to note that the final state classification discussed here should not be dramatically affected when relaxing the hypothesis of section 2.1, e.g. in models where the \tilde{g} are lighter than the \tilde{q} , or where the LSP is the χ_1^+ .

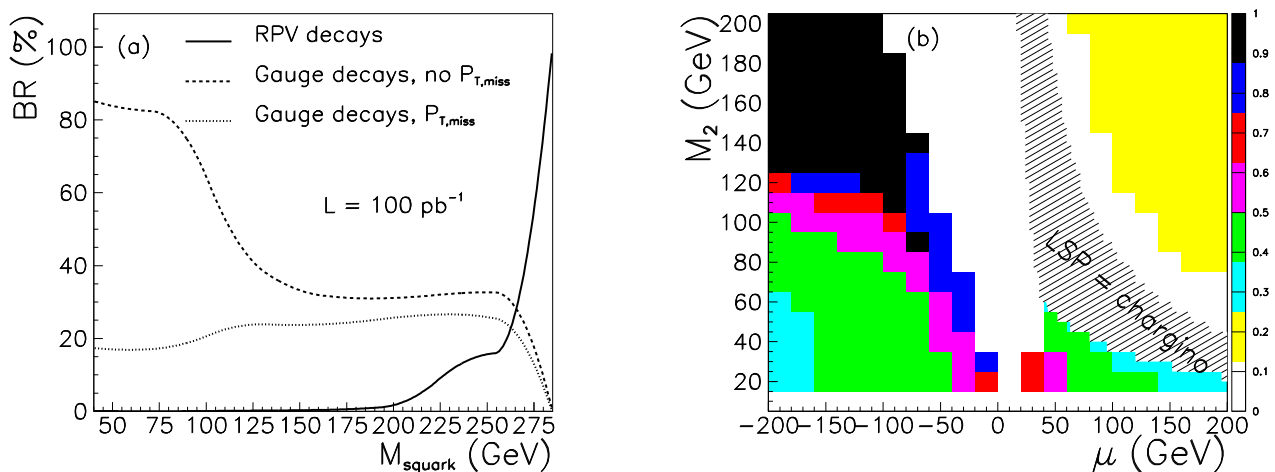


Figure 10: (a) *Squark decay branching ratio as a function of squark mass integrated over three distinct set of event topologies for $\tan\beta = 1$ and $M_{\tilde{\gamma}} = 40$ GeV. (b) Ratio $\mathcal{B}_{S4}/\mathcal{B}_{S3}$ of the squark “gauge” decay branching ratios without \cancel{P}_\perp involving the like ($S3$) and unlike ($S4$) sign lepton viewed in the M_2 versus μ plane; the plot is obtained for $M_{\tilde{q}} = 150$ GeV at the expected limit of λ' coupling sensitivity for an integrated HERA luminosity of 100 pb^{-1} .*

Assuming $M_{\tilde{g}} < M_{\tilde{q}}$, the decay $\tilde{q} \rightarrow q + \tilde{g}$ will generally dominate. If the \tilde{g} is the LSP, the \tilde{q} decay will be followed by the \tilde{R}_p decay $\tilde{g} \rightarrow q + q' + e^\pm$ or $\tilde{g} \rightarrow q + \bar{q} + \nu$. In such a case, possible final states contain several jets and either one electron or \cancel{P}_\perp . These topologies correspond to channels **S3** and **S5**, previously considered. If $M_{\tilde{q}} > M_{\tilde{g}}$, with the LSP being the lightest neutralino, the \tilde{g} arising from squark decay will undergo $\tilde{g} \rightarrow q + \tilde{q}$, the latter squark being off-shell. Possible final states are similar to those listed above, but more jets would be expected. Assuming now that the LSP is the χ_1^+ (see the relevant MSSM parameters in Fig. 3b), a new event topology would only emerge for a relatively stable χ_1^+ which could behave as a ‘‘heavy muon’’. However, the time of flight of the χ_1^+ , obtained from the integration (13) over phase space, reads as :

$$\tau = \frac{4\pi}{g^2} \frac{1}{|V_{11}|^2} \frac{1}{\lambda'^2} (8 \times 64\pi^2) \left(\frac{M_{\tilde{q}}}{M_{\chi_1^+}} \right)^4 \frac{1}{M_{\chi_1^+}} \quad (14)$$

which numerically leads to :

$$\tau = (2.5 \cdot 10^{-15} \text{ s}) \left(\frac{5 \cdot 10^{-3}}{\lambda'} \right)^2 \frac{1}{|V_{11}|^2} \left(\frac{100 \text{ GeV}}{M_{\chi_1^+}} \right)^5 \left(\frac{M_{\tilde{f}}}{150 \text{ GeV}} \right)^4. \quad (15)$$

From this formula one obtains that the relevant parameter space for the χ_1^+ to decay outside the detector ($\gtrsim 1\text{m}$), is already excluded from the intrinsic Z^0 width measurement at CERN [18].

3 Results for the Mass-Coupling Reach of HERA

In the absence of a significant deviation from the SM expectations, exclusion limits for the Yukawa couplings λ'_{1jk} as a function of mass can be derived, showing the domain HERA could probe in the near future. Results are shown for λ'_{1j1} in Fig. 11 at 95% confidence level (CL), for integrated luminosities $L = 100\text{pb}^{-1}$ and $L = 500\text{pb}^{-1}$. These have been obtained assuming a 40 GeV $\tilde{\gamma}$ -like χ_1^0 , and combining all contributing channels. For $\mathcal{L} = 500\text{pb}^{-1}$, the existence of first generation squarks with \tilde{R}_p Yukawa coupling λ'_{1j1} could be excluded for masses up to ~ 270 GeV for coupling strengths $\lambda_{111}^2/4\pi \gtrsim \alpha_{em}$.

From the analysis of the λ'_{1j1} case involving the \tilde{d}_R and \tilde{u}_L squarks, limits can be deduced on the λ'_{1jk} by folding in the proper parton densities. Such limits are given in Table 4 at $M_{\tilde{q}} = 150$ GeV and for an integrated luminosity of 500pb^{-1} . Also quoted in this table are the most severe existing indirect limits for each of these couplings. The most stringent concern couplings λ'_{1jk} with $j = k$ and come either from the non-observation of neutrinoless double-beta decay ($j = k = 1$) or from constraints on the ν_e mass ($j = k = 2, 3$). The limit from $\beta\beta 0\nu$ decay depends on the gluino mass and is given here for $M_{\tilde{g}} = 500$ GeV.

By the time HERA reaches high luminosity running conditions, new direct limits (or a discovery !) from other colliders will have further constrained the possible squark masses and SUSY parameters. In e^+e^- collisions, the direct squark pair production process does not violate R-parity and LEP2 should directly probe squark masses up to $\sqrt{s}/2$, i.e. $\simeq 90$ GeV. In $p\bar{p}$ collisions, squarks can be produced in pair or in association with gluinos. No complete analysis in the \tilde{R}_p -SUSY framework has been performed yet with existing TEVATRON data. Nevertheless, \tilde{q} decay topologies similar to those described here have been explored by D0 [25] and CDF [26] in scalar leptoquark or MSSM searches. From these and from di-lepton data [27],

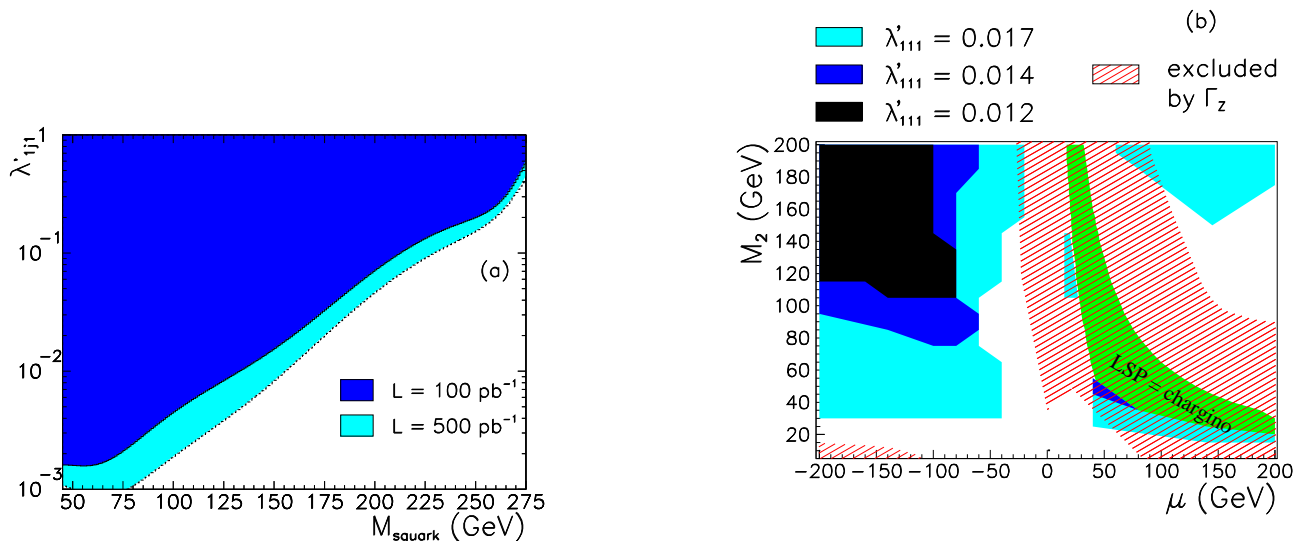


Figure 11: (a) Exclusion upper limits at 95% CL on the λ'_{1j1} coupling as a function of squark mass which could be reached with e^+p collisions at HERA ($\sqrt{s} \sim 300$ GeV) for integrated luminosities of $L = 100 \text{ pb}^{-1}$ (dark shaded area) and 500 pb^{-1} (shaded); (b) Regions of the M_2 versus μ plane excluded for $L = 100 \text{ pb}^{-1}$ and for couplings λ'_{1j1} equal or smaller to the exclusion upper limit at $M_{\tilde{q}} = 150$ GeV.

Table 4: Exclusion upper limits at 95% CL on the coupling λ'_{1jk} for $M_{\tilde{q}} = 150$ GeV and $M_{\chi_1^0} = 40$ GeV together with best existing indirect limits. The indirect limits have been scaled from those found in the cited references to $M_{\tilde{q}} = 150$ GeV and 95% CL.

	HERA sensitivity		Indirect limits	
	$\tilde{\gamma}$ -like χ_1^0	\tilde{Z} -like χ_1^0	Value [Ref.]	Nature of the process
λ'_{111}	0.008	0.023	0.003 [19]	$\beta\beta 0\nu$ decay
λ'_{112}	0.020	0.057	0.05 [20]	CC-universality
λ'_{113}	0.026	0.072	0.05 [20]	CC-universality
λ'_{121}	0.008	0.023	0.09 [21]	Atomic Parity Viol.
λ'_{122}	0.027	0.077	0.04 [22]	ν_e -mass
λ'_{123}	0.043	0.012	0.5 [23]	$D^+ \rightarrow K$ decays
λ'_{131}	0.007	0.024	0.09 [21]	Atomic Parity Viol.
λ'_{132}	0.027	0.091	0.77 [24]	R_e^{exp}
λ'_{133}	0.068	0.230	0.0015 [22]	ν_e -mass

one can infer that the range $200 \rightarrow 300$ GeV of \mathcal{R}_p -SUSY squark masses will most probably be not fully excluded by TEVATRON data for an integrated luminosity of $\sim 100 \text{ pb}^{-1}$, thus leaving open a discovery window at HERA in the hypothesis $M_{\tilde{g}} \gg M_{\tilde{q}}$.

If the presence of two simultaneously non-vanishing Yukawa couplings (e.g. λ'_{1jk} and λ'_{ijk} with $i \neq 1$), resonant \tilde{q} production at HERA can be directly followed by a lepton flavor violation (LFV) decay leading to $\mu + \text{jet}$ or $\tau + \text{jet}$ signatures. Relevant analysis with existing data have been performed by the H1 [13] and ZEUS [28] collaborations and limits comparable to the best existing indirect LFV limits have been derived in the context of \mathcal{R}_p -SUSY for a pure $\tilde{\gamma}$ like LSP.

A new range of possible coupling products could be probed with increasing luminosity [29].

4 Summary and Conclusions

The HERA potential for R -parity violating supersymmetry searches was studied. Direct resonant production of squarks through nine new Yukawa couplings λ'_{1jk} is possible up to the kinematical limit of ~ 300 GeV.

Supersymmetric partners \tilde{q}_L of left handed u -like squarks are produced preferentially in e^+p collisions and most favourably via λ'_{1j1} . In contrast, e^-p collisions mainly produce partners \tilde{q}_R of right-handed d -like quarks and most favourably via λ'_{11k} . Squark decays via a λ' coupling into $l + q$ final states dominate only at largest accessible masses, while elsewhere squarks undergo mainly gauge decays into a quark and a gaugino-higgsino. The \tilde{q}_R decays involve a neutralino χ^0 while \tilde{q}_L decays dominantly proceed via a chargino χ^\pm in a large portion of the MSSM parameter space. The χ 's, including the LSP, are generally unstable and their decay chain involves the λ'_{1jk} coupling.

In total, eight classes of event topologies are identified for R -parity and gauge decays of squarks, with single or multi-leptons final states accompanied or not by missing transverse momenta. A good experimental sensitivity is expected in each of these classes. Thus, for an integrated luminosity of 500 pb^{-1} , squarks can be searched for Yukawa couplings smaller than the electromagnetic coupling up to masses of $\lesssim 270$ GeV, almost independently of the specific choice of MSSM parameter values. Coupling values below the most stringent indirect limits can be probed at $M_{\tilde{q}} = 150$ GeV for seven out of the nine possible λ'_{1jk} couplings.

References

- [1] For reviews on Supergravity see
P. Van Nieuwenhuizen, Phys. Rep. 68 (1981) 189 or H.P. Nilles, Phys. Rep. 110 (1984) 1 and references therein.
- [2] The “hierarchy” and “naturalness” problems are reviewed in
L.E. Ibáñez and G.G. Ross, Perspectives on Higgs Physics, G. Kane (Editor) World Scientific (1993) and references therein.
- [3] For a phenomenological review see for instance
H.E. Haber and G.L. Kane, Phys. Rep. 117 (1985) 75.
- [4] L.J. Hall and M. Suzuki, Nucl. Phys. B231 (1984) 419; S. Dawson, Nucl. Phys. B261 (1985) 297; S. Dimopoulos and L.J. Hall, Phys. Lett. B207 (1987)210.
- [5] L.E. Ibáñez and G.G. Ross, Nucl. Phys. B368 (1992) 3.
- [6] A. Nelson and S. Barr, Phys. Lett. B246 (1990) 141; H. Dreiner and G.G. Ross, Nucl. Phys. B410 (1993) 188.
- [7] J. Butterworth and H. Dreiner, Proceedings of the Workshop Physics at HERA, W. Buchmüller, G. Ingelman (Editors), DESY Hamburg (October 1991) p1079; Idem, Nucl. Phys. B397 (1993) 3.

- [8] H1 Collaboration, T. Ahmed et al., *Z. Phys.* C64 (1994) 545.
- [9] E. Perez and Y. Sirois, *Proceedings of the International Workshop on Supersymmetry and Unification of Fundamental Interactions*, Editions Frontières, I. Antoniadis and H. Videau (Editors), Palaiseau, France (May 1995) p21; Y. Sirois, *Proceedings of the 4th International Conference on Supersymmetries in Physics*, R. Mohapatra (Editor) College Park, Maryland, USA (May 1996).
- [10] E. Perez, “Recherche de Particules en Supersymétrie Violant la R-parité dans H1 à HERA”, Thèse de Doctorat, DAPNIA/SPP report 96-1008 (in French).
- [11] H1 Collaboration, S. Aid et al., *Z. Phys.* C71 (1996) 211.
- [12] H. Dreiner, P. Morawitz, *Nucl. Phys.* B428(1994) 31.
- [13] H1 Collaboration, S. Aid et al., *Phys. Lett.* B369 (1996) 173.
- [14] W. Buchmüller, R. Rückl and D. Wyler, *Phys. Lett.* B191 (1987) 442.
- [15] J.F. Gunion, H.E. Haber, *Nucl. Phys.* B272 (1986) 1.
- [16] A. Bartl, H. Fraas, W. Majerotto and B. Mosslächer, *Z. Phys.* C55 (1992) 257.
- [17] E. Perez, on behalf of H1 and ZEUS Collaborations, to be published in the proceedings of the XXVIIIth International Conference on High Energy Physics, World Scientific (Editor), Warsaw (25-31 July 1996).
- [18] ALEPH Collaboration, D. Buskulic et al., *Phys. Lett.* B349 (1995) 238.
- [19] M. Hirsch, H.V. Klapdor-Kleingrothaus, S.G. Kovalenko, *Phys. Rev. Lett.* 75 (1995) 17.
- [20] V. Barger, G.F. Giudice, T. Han, *Phys. Rev.* D40 (1989) 2987.
- [21] S. Davidson, D. Bailey, B. A. Campbell, *Z. Phys.* C 61 (1994) 613, hep-ph/9309310.
- [22] R. Godbole, P. Roy, X. Tata, *Nucl. Phys.* B401 (1993) 67.; S. Dimopoulos, L.J. Hall, *Phys. Lett.* B207 (1987) 210.
- [23] G. Bhattacharyya, D. Choudhury, *Mod. Phys. Lett.* A10 (1995) 1699.
- [24] G. Bhattacharyya, J. Ellis, K. Sridhar, *Mod. Phys. Lett.* A10 (1995) 1583.
- [25] D0 Collaboration, S. Abachi et al., *Phys. Rev. Lett.* 75 (1995) 618.
- [26] CDF Collaboration, F. Abe et al., *Phys. Rev. Lett.* 75 (1995) 613.
- [27] M. Guchait, D.P. Roy, *Phys. Rev.* D54 (1996) 3276; H. Dreiner, M. Guchait and D.P. Roy, *Phys. Rev.* D49 (1994) 3270.
- [28] ZEUS Collaboration, M. Derrick et al., Preprint DESY-96-161 (Aug. 1996), 38 pp.
- [29] F. Sciulli and S. Yang, Contribution to this Workshop.

Appendix: Gaugino-higgsino mixing

Detailed expressions (and conventions) used for the mass mixing in the gaugino-higgsino sector are presented here for completeness.

Neutralino mass mixing:

Mass terms of the Lagrangian describing $SU(2)_L \times U(1)_Y$ neutral gauginos and higgsinos can be written as :

$$\mathcal{L}_m = -1/2(\psi_i^0)^T Y^{ij} \psi_j^0 + h.c. \quad (16)$$

where the neutralino mass matrix in the basis $\psi_i^0 = (-i\tilde{A}, -i\tilde{W}_3, \tilde{H}_1^0, \tilde{H}_2^0)$ is given by :

$$Y = \begin{pmatrix} M_1 & 0 & -m_Z \sin \theta_W \cos \beta & m_Z \sin \theta_W \sin \beta \\ 0 & M_2 & m_Z \sin \theta_W \cos \beta & -m_Z \cos \theta_W \sin \beta \\ -m_Z \sin \theta_W \cos \beta & m_Z \cos \theta_W \cos \beta & 0 & -\mu \\ m_Z \sin \theta_W \sin \beta & -m_Z \cos \theta_W \sin \beta & -\mu & 0 \end{pmatrix} \quad (17)$$

The number of free MSSM parameters is reduced by using a GUT inspired relation between soft-breaking terms M_1 and M_2 , $M_1 = \frac{5}{3} \tan^2 \theta_W M_2$.

Neutralinos correspond to the mass eigenstates and are defined as $\chi_i^0 = N^{ij} \psi_j^0$, with N_{ij} being the unitary matrix which diagonalize Y . Finally, we make use of the matrix N' , which diagonalizes the neutralino mass matrix expressed in the basis $(\tilde{\gamma}, \tilde{Z})$ instead of (\tilde{A}, \tilde{W}_3) : $N'_{j1} = N_{j1} \cos \theta_W + N_{j2} \sin \theta_W$, $N'_{j2} = -N_{j1} \sin \theta_W + N_{j2} \cos \theta_W$, $N'_{j3} = N_{j3}$ and $N'_{j4} = N_{j4}$.

Chargino mass mixing:

The Lagrangian mass terms for winos and charged higgsinos are written as :

$$\mathcal{L}_m = -\frac{1}{2}(\psi^+, \psi^-) \begin{pmatrix} 0 & X^T \\ X & 0 \end{pmatrix} \begin{pmatrix} \psi^+ \\ \psi^- \end{pmatrix} + h.c. \quad (18)$$

where :

$$X = \begin{pmatrix} M_2 & m_W \sqrt{2} \sin \beta \\ m_W \sqrt{2} \cos \beta & \mu \end{pmatrix} \quad (19)$$

and $\psi_j^+ = (-i\tilde{W}^+, \tilde{H}_2^+)$, $\psi_j^- = (-i\tilde{W}^-, \tilde{H}_1^-)$. This mass matrix is diagonalized using two (2, 2) unitary matrices U and V [16] : $\chi_i^+ = V^{ij} \psi_j^+$ and $\chi_i^- = U^{ij} \psi_j^-$. Masses for these eigenstates are easily derived from the above X matrix :

$$M_{1,2}^2 = \frac{1}{2}(M_2^2 + \mu^2 + 2m_W^2 \mp [(M_2^2 - \mu^2)^2 + 4m_W^4 \cos^2 2\beta + 4m_W^2(M_2^2 + \mu^2 + 2M_2\mu \sin 2\beta)]^{1/2}) \quad (20)$$

